Journal of Visualization, Vol. 7, No. 1 (2004) 25-32

Stereoscopic PIV Measurements of Flow around a Marine Propeller

Lee, S. J.*[1] and Paik, B. G.*[2]

*1 Department of Mechanical Engineering, Pohang University of Science and Technology, San 31, Hyo-Ja Dong, Pohang, 790-784, Korea.
E-mail: sjlee@postech.ac.kr
*2 Department of Mechanical Engineering, Pohang University of Science and Technology, San 31, Hyo-Ja Dong, Pohang, 790-784, Korea.

Received 1 March 2003
Revised 7 August 2003

Abstract : A stereoscopic PIV (Particle Image Velocimetry) technique has been employed to measure the 3 dimensional flow structure of turbulent wake behind a marine propeller with 5 blades. The out-of-plane velocity component was measured using particle images captured simultaneously by two CCD cameras installed in the angular displacement configuration. 400 instantaneous velocity fields were acquired for each of four different blade phases of 0°, 18°, 36° and 54°. They were ensemble averaged to investigate the spatial evolution of propeller wake in the near wake region up to one propeller diameter (D) downstream. The phase-averaged velocity fields show clearly the viscous wake formed by the boundary layers developed along both surfaces of the blade. Tip vortices were generated periodically and the slipstream contraction occurs in the near-wake region. The out-of-plane velocity component has large values at the locations of tip and trailing vortices. With going downstream, the axial turbulence intensity and the strength of tip vortices were decreased due to the viscous dissipation, turbulence diffusion and blade-to-blade interaction. The difference in the mean velocity fields measured by SPIV and 2-D PIV methods was about 5% ~ 10%. However, the 2-D PIV results also give sufficient information on propeller wake beyond the region of X/D = 0.2.

Keywords : Stereoscopic PIV(SPIV), Propeller wake, Tip vortex, Wake sheet

1. Introduction

Larger and faster marine vehicles have been designed to have heavy loading on propeller blades. However, the increase of propeller loading may cause some problems such as noise, hull vibration, and cavitation at high speed. The geometry of a propeller should be optimized to solve these problems. Generally a modern propeller blade has a complicated geometry, making the wake behind a propeller more complicated. Therefore, the reliable wake analysis based on detailed experimental measurements can give useful information to optimize the geometrical shape of a propeller.

The marine propeller performance has been studied by many researchers using the potential-based panel method. However, the numerical analysis needs adequate wake sheet modeling based on the experimental data or special theory to yield a satisfactory prediction for the formation of tip or trailing vortices. In addition, it is very important to predict the strength and trajectory of the tip vortices inducing energy loss in propulsion, hull vibration and noise. The actual vortex sheet of wake has been assumed as a thin filament in the numerical analysis. Therefore, more

accurate flow information based on reliable experiments is required for the supplement on numerical calculation together with the development of viscous codes.

The propeller wake has been usually measured using point-wise experimental techniques such as hot film, Pitot tube and LDV (Laser Doppler Velocimetry), measuring flow velocities at discrete points by scanning the flow field with an array of velocity probes. Stella et al. (1998) measured the axial velocity component of a propeller wake, and Chesnakas and Jessup (1998) investigated the tip vortices using LDV. The point-wise methods unfortunately take long time to acquire sufficient data, especially to obtain the phase-averaged velocity information.

Velocity field measurement techniques have been employed to measure the flow around a marine propeller. The PIV (particle image velocimetry) technique has merits of non-intrusiveness and simultaneous whole field measurements. Another merit is very short measuring time to obtain the phase-averaged velocity fields compared with point-wise measuring technique. Controni et al. (2000) investigated the near-wake behind a marine propeller in a cavitation tunnel using a PIV technique. They showed the spatial evolution of wake structure in the longitudinal plane. Lee et al. (2002) investigated the propeller wake up to 2 propeller diameter downstream regions in the longitudinal plane using a hybrid PTV (Particle Tracking Velocimetry) method. They found similar wake structure in good spatial resolution, compared with the previous results.

Stereoscopic PIV (SPIV) technique has been used widely to investigate 3-D (three dimensional) flow structure where accurate flow analysis is needed. Conventional 2-D PIV technique using a single camera supplies only in-plane velocity field information. The out-of-plane motion is embedded into the in-plane velocity field data and becomes a source of measurement error in 2-D PIV measurements. Therefore, 2-D PIV results measured for 3-D flows may have some perspective errors caused by the out-of-plane velocity component. The SPIV technique employed in this study uses two cameras and each camera captures the same instantaneous particle image field at different angles. Intermediate procedures of SPIV technique provide 3-D velocity fields using 2-D particle displacement information obtained from the flow images captured by each camera.

Soloff et al. (1997) developed a SPIV calibration method that does not require the geometry information during the reconstruction procedure. They measured calibration data at three different locations parallel to the object plane and obtained a non-linear mapping function, providing the relationship between 3-D object field and 2-D image field for each camera. The particle displacements were measured using this mapping function. Yoon & Lee (2002) measured the flow around an axial fan using a SPIV technique with a 3-D calibration method. They compared directly the in-plane velocity fields and local turbulence intensity distributions measured by 2-D PIV method with the 3-D SPIV results. They obtained about 2.7% and 5.8% maximum differences caused by the out-of-plane motion, respectively. Recently, Calcagno et al. (2002) investigated 3-D wake behind a propeller in the transverse plane using a SPIV technique and showed spatial evolution of propeller wake.

The main objectives of present study are to illustrate the usefulness of the SPIV technique in analyzing a complex 3-D flow behind a marine propeller and to investigate the flow characteristics of propeller wake in detail. In addition, the contribution of out-of-plane motion embedded in 2-D PIV results on 3-D propeller wake was investigated with direct comparison of 2-D PIV and SPIV results. The spatial distributions of three orthogonal velocity components of near-wake behind a marine propeller were measured in the longitudinal plane. Four hundred instantaneous velocity fields were measured at four different phases of the propeller blade and phase-averaged to get the spatial evolution of flow structure and turbulence statistics.

2. Basic Principle of SPIV

Angular configuration where the two optical axes are neither parallel nor perpendicular to the measurement plane was employed for the SPIV measurements. The angular displacement method

requires the image planes to be tilted at some angle to the object plane to focus the whole measuring volume. The tilting of the image planes, camera lenses and CCD sensor result in optical aberrations and particle image distortion, causing non-uniform magnification. Due to the image distortion and magnification variation, a sophisticated calibration process and a small aperture should be used to obtain accurate flow data.

When the ray tracing method is used with the angular configuration, it is needed to derive the geometric relationship between the real particle displacements $\Delta\underline{\mathbf{x}} = (\Delta x, \Delta y, \Delta z)$ and the projected displacements $\Delta\underline{\mathbf{X}} = (\Delta X_1, \Delta Y_1, \Delta X_2, \Delta Y_2)$ in the image-recording plane. The geometric relationship between the two displacements in the image plane can be described as follows.

$$\Delta X_1 = a_1\Delta x + a_2\Delta z \quad (1)$$
$$\Delta Y_1 = a_3\Delta y + a_4\Delta z \quad (2)$$
$$\Delta X_2 = a_5\Delta x + a_6\Delta z \quad (3)$$
$$\Delta Y_2 = a_7\Delta y + a_8\Delta z \quad (4)$$

The four equations for three unknown particle displacements (Δx, Δy and Δz) are derived from the geometric relationship between the object plane and the camera planes. These equations can be solved with a least square method or reduction of equation numbers by averaging two equations with the assumption that Y-axis of each camera is parallel to the Y coordinate of the physical domain.

However, the aberrations due to variations in refractive index and particle image distortion may generate the non-uniformity in magnification. These image distortion and optical aberration were compensated by employing the calibration procedure developed by Soloff et al. (1997). The relation between 3-D object volume and 2-D image planes of two cameras can be written as

$$\underline{\mathbf{X}} = F(\underline{\mathbf{x}}) \quad (5)$$

Here, $\underline{\mathbf{X}} = (X_1, Y_1, X_2, Y_2)$ is the projected image position and $\underline{\mathbf{x}} = (x, y, z)$ is the real particle location in the object volume. The mapping function F can be expressed as a polynomial form. Since Y-axes of two CCD cameras are parallel to the Y coordinate of the physical space, the displacement equations for the Y direction in the two consecutive image planes are averaged not to bear over-determined solution in the calibration procedure.

3. Experimental Apparatus and Method

The propeller wake was measured in circulating water channel with a test section size of $120^{L}\times30^{W}\times20^{H}$ cm^3. Figure 1 shows the geometry and specification of propeller KP505 for the 3600TEU container vessel tested in this study. The propeller of 54mm in diameter has 5 blades with a design advance coefficient J of 0.72. The free stream velocity was fixed to 32.5 cm/s and the Reynolds number based on the propeller diameter is about 18000. The field of view for PIV measurement was 6×6 cm^2.

Figure 2 shows the SPIV system consisting of a dual-head Nd:YAG laser, two CCD cameras with a stereoscopic lens, a synchronizer, a motor controller and an IBM PC. The Nd:YAG laser has a pulse width of about 7 ns with energy of 125 mJ per pulse. The two CCD cameras have the spatial resolution of 1024×1024 pixels. The measurement plane was illuminated by thin laser light sheet from the bottom of water channel. The scattered particle images were captured by two CCD cameras for velocity field measurements. The CCD cameras and laser were synchronized with the angular position of the propeller blade. The 3-D velocity components (axial velocity u, vertical velocity v and out-of-plane velocity component w) can be extracted from two consecutive particle images captured from left and right cameras of SPIV system.

Silver coated hollow glass beads with mean diameter of 10μm were used as seeding particles. A servo-motor attached with an encoder was used to derive the propeller. The propeller was installed at the depth sufficient to neglect the free surface effect. A support strut was installed to prevent the surge or vibration of the propeller shaft. The propeller was driven from downstream to avoid the

effect of wake generated from the supporting strut. The propeller wake could not be measured along the center axis due to the presence of propeller shaft in the downstream region. The encoder mounted on the servo-motor generates trigger signals to synchronize laser and CCD cameras with an accuracy of 0.36° for each angular position. The encoder signals were low-pass filtered to get a clear trigger signal. The time interval between two consecutive particle images was set to 300μs, for which the propeller rotates 0.9°. The velocity field measurements were carried out at four different phases (ϕ = 0°, 18°, 36°, 54°) with the angular interval of 18° between two adjacent measurement phases.

Most errors in SPIV measurements result from the wrong evaluation of particle displacement that is usually less than 1/10th of a pixel for current PIV algorithm(Raffel et al, 1998), equivalent to 1.95cm/s approximately. The measurement error for the out-of-plane velocity component was evaluated to be about 5%, as mentioned in the direct comparison of the SPIV method employed in this study and 2-D PIV(Yoon & Lee, 2002).

Four hundred instantaneous velocity fields were obtained for each blade phase. Mean velocity fields, vorticity distribution and turbulence statistics such as turbulence intensity were obtained by ensemble-averaging the instantaneous velocity fields to investigate the spatial evolution of the wake structure according to blade phase.

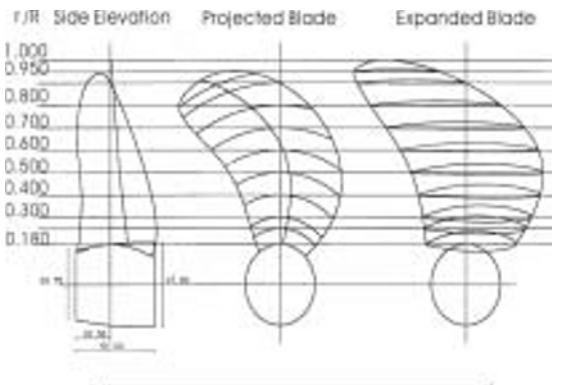

Specification of Kp505 propeller model			
DIAMETER(MM)	: 54.0	SCALE RATIO	: 146.3
(P/D) mean	: 0.950	PROP. TYPE	: FPP
Ae/Ao	: 0.800	SECTION	: NACA66
HUB RATIO	: 0.180	NO. OF BLADES: 5	

Fig. 1. The geometry and specification of propeller model.

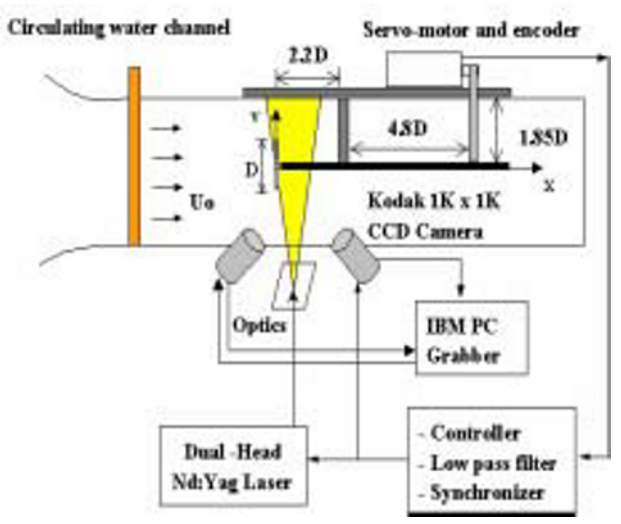

Fig. 2. Schematic diagram of experimental set-up with SPIV system.

4. Results and Discussion

The contour plots of phase-averaged axial velocity at phase angle ϕ = 0° are shown in Fig. 3. The positive X-axis and Y-axis normalized by the propeller diameter D indicate the direction of main flow and vertical upwardness, respectively. The tip of blade is located at X/D = 0 and Y/D = -0.5. A slipstream is formed in the region between the propeller shaft and the propeller tip. The slipstream has larger axial velocity compared with that of free stream because the propeller rotation supplies axial momentum. The velocity deficits occur near the locations of blade tip and propeller shaft, indicating the presence of viscous wake. The viscous wake takes place in the near-wake due to the merging of two boundary layers developed on the pressure and suction sides of propeller blade.

Figure 4 shows the contour of phase-averaged spanwise vorticity at ϕ = 0°. The wake sheets and tip vortices are generated periodically from the blade tips in the region around the depth of Y/D= -0.5. Tip vortices evolve downstream periodically with a regular spacing. Tip vortex generated from

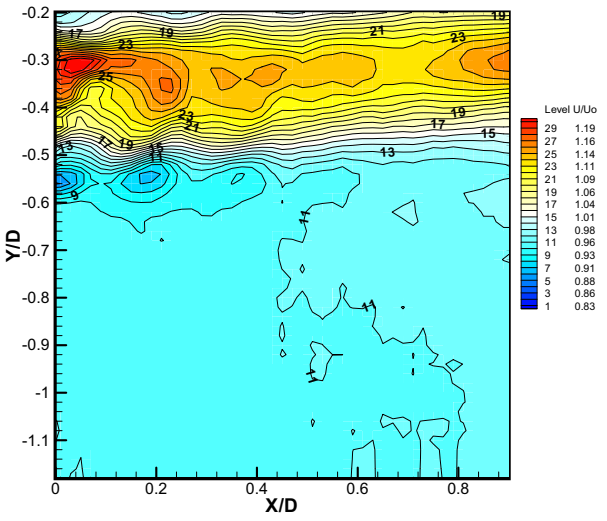

Fig. 3. Contour plots of phase-averaged axial velocity at ϕ = 0º.

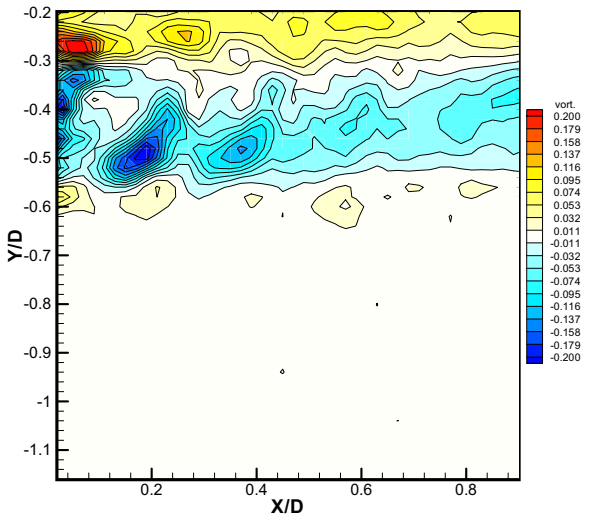

Fig. 4. Contour plots of phase-averaged spanwise vorticity at ϕ = 0º.

the difference of tangential velocity between upper and lower surfaces of a propeller blade rolls up from a vortex sheet. The trailing vortices come from the trailing edge of a propeller blade are composed of two vortex sheets with opposite sign, because two boundary layers are developed along the upper and lower blade surfaces. The shape of tip vortices is skewed up in the region up to X/D=0.5. This asymmetry shape of tip vortices seems to be caused by strong interaction between tip vortices and wake sheet. As the flow goes downstream, the asymmetry is decreased because the interaction between tip vortex and wake sheet attenuates. The trace of tip vortices contracts toward the propeller shaft up to the region of X/D=0.5, thereafter it is contracted more due to the blade-to-blade interaction up to the region of X/D=1.0. The contraction of slipstream tip vortex trajectory over the region of X/D=0.5 seems to be result from the blade-to-blade interaction. The slipstream toward the propeller shaft continues up to the region of 1D downstream. The blade wake within the slipstream being faster than the projection of tip vortices in the axial direction seems to interact with the tip vortex generated from the previous blade.

In order to investigate flow characteristics of propeller wake due to the out-of-plane flow motion, the out-of-plane velocity component (w) was represented in a 3-D vector plot as shown in Fig. 5. The wake sheet including trailing vortices seems to be generated within the propeller slipstream region of $-0.5 < X/D < 0$. In addition, the out-of-plane velocity component has large values along the trailing vortices in the wake sheet. However, the in-plane motion is dominant outside the slipstream. In the very near wake region of $X/D < 0.2$, the magnitude of out-of-plane velocity component is about 17% larger than free stream velocity. However, as the wake goes downstream, the out-of-plane velocity component is decreased gradually. Its magnitude is only about 10% of free stream velocity at X/D=1 downstream location. Due to strong out-of-plane motion, 2-D PIV technique can cause some errors in propeller wake measurement in $X/D < 0.2$. The non-axial flow motion indicates that some of the propulsion energy is consumed ineffectively. Therefore, the out-of-plane velocity component w together with the strength of tip vortices can be used as a control parameter to optimize the propeller design.

Figure 6 shows the phase-to-phase variation of the out-of-plane velocity component at the locations of tip vortices. As the flow goes downstream, the out-of-plane velocity component at tip vortices reduces gradually beyond the downstream location of X/D=0.2. The gradual decrease seems to be caused by viscous dissipation, turbulent diffusion and blade-to-blade interaction. Its magnitude is about 8% ~ 13% of free stream velocity in near-wake region. The out-of-plane velocity component may contribute as a main source of perspective errors, overestimating slightly the in-plane velocity field.

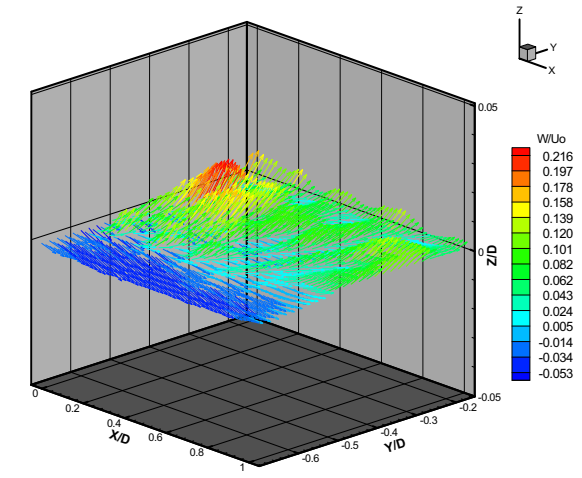

Fig. 5. Three dimensional velocity vector plots at phase angle of ϕ = 0º.

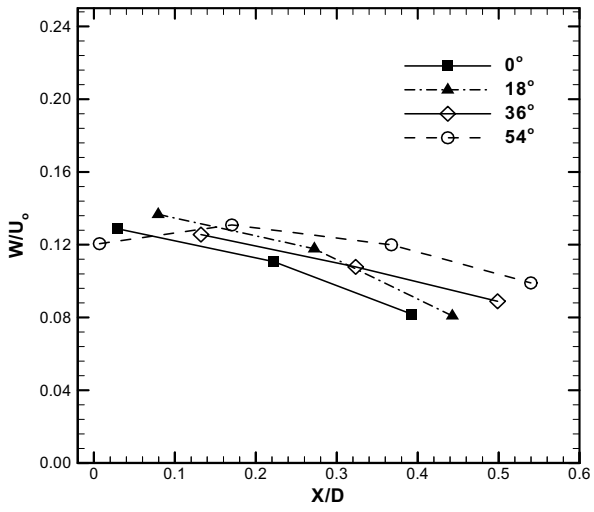

Fig. 6. Phase-to-phase variation of out-of-plane velocity component.

Figure 7 represents the turbulence intensity distribution of axial velocity components ($\sqrt{u'^2}/U_o$) normalized by the free stream velocity U_0. The axial turbulence intensity has locally high values along the trace of tip and trailing vortices, compared with the other wake region. The flow interaction between the tip vortices and the wake sheet transports the axial turbulence intensity to far downstream region. The tip and trailing vortices and rotational flow motion of propeller wake generate large turbulence intensity. The variation of axial turbulence intensities at the locations of tip vortices is shown in Fig. 8. As the flow goes downstream, the axial turbulence intensity decreases in the near-wake region and converges gradually to a value of free stream due to the viscous dissipation and turbulent diffusion. As the phase angle ϕ increases, the axial turbulence intensity is increased. The turbulence production may be attributed to the blockage effect of flow passage by the propeller blade at ϕ = 36° and 54°.

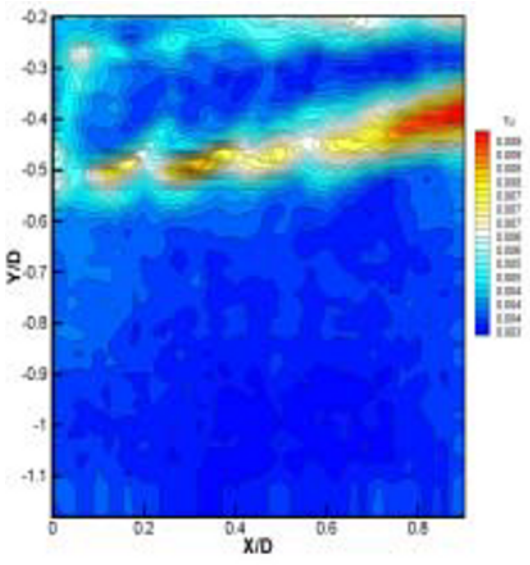

Fig. 7. Axial turbulence intensity distribution.

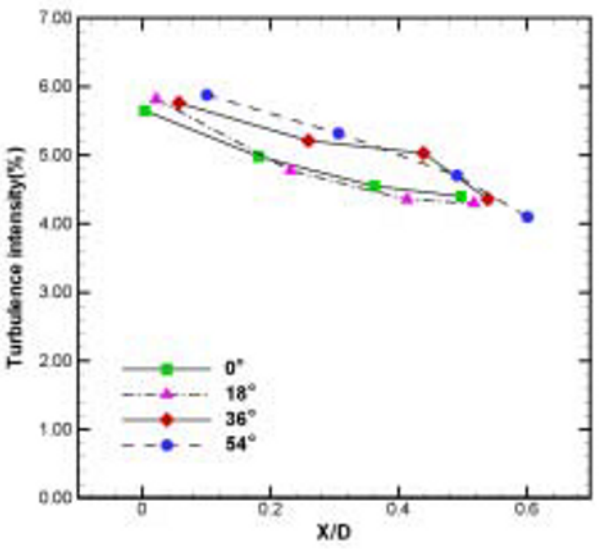

Fig. 8. Phase-to-phase variation of axial turbulence intensity.

The spatial distributions of in-plane mean velocity and turbulence intensity measured by 3-D SPIV method were compared with 2-D PIV method. Even though they were not measured simultaneously, the experimental conditions such as camera resolution, free stream speed, field of view and propeller revolution were identical. The maximum differences of the free stream velocity and propeller revolution measured by the two methods are about 0.5% and 0.2%, respectively. The in-plane velocity fields measured by two different methods show similar flow pattern. However, the physical quantities show more or less some differences in their magnitude. The axial mean velocity difference in which the 2-D PIV result was subtracted by the corresponding result measured by 3-D SPIV method is shown in Fig. 9(a). In the region of tip and trailing vortices, the difference is about 5% ~ 10% on average and the maximum error is about 20% at the first tip vortex located near X/D = 0.2. The difference in the axial turbulence intensity distributions of axial velocity component between 2-D and 3-D PIV measurements is also large as shown in Fig. 9(b). The axial turbulence intensity distribution measured by 2-D PIV method is overestimated due to the out-of-plane velocity component. The difference is about 10% ~ 15% at the location of trailing vortices in the near-wake region just behind the propeller. From these results, we can see that relatively large errors are embedded in the in-plane velocity fields measured by 2-D PIV method in the near-wake region just behind a rotating propeller where the out-of-plane velocity component has high values. However, the conventional 2-D PIV method seems to be applicable to analyze the propeller wake beyond the region of X/D = 0.2 where the perspective error is relatively small. In some sense, the flow field analysis of propeller wake using a 2-D PIV systems may be helpful for engineering diagnosis such as initial design or relative comparison of marine propellers.

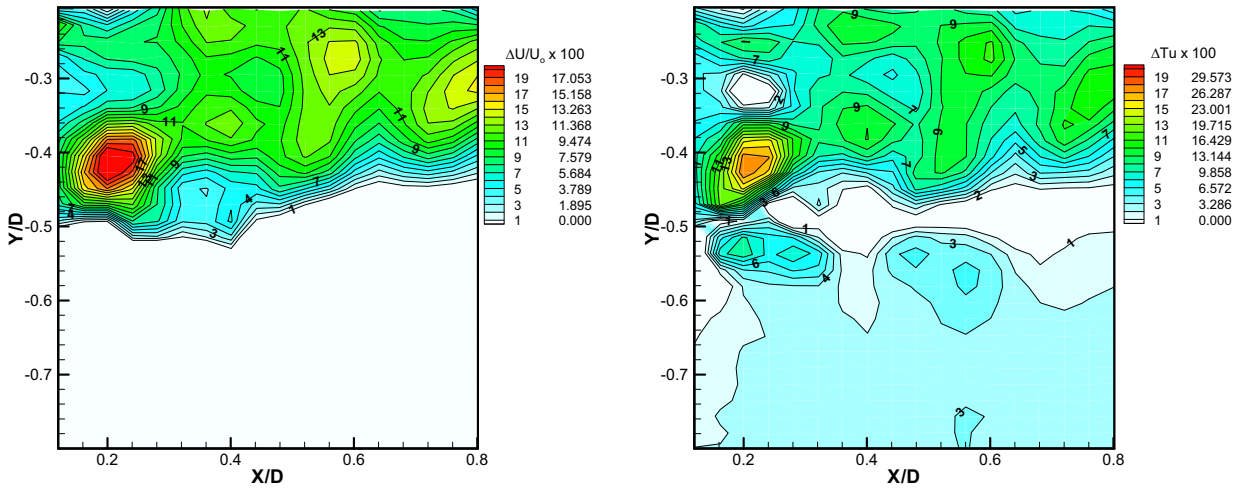

(a) axial mean velocity (b) axial turbulence intensity

Fig. 9. Direct comparison of axial mean velocity and axial turbulence intensity measured by SPIV and 2-D PIV methods.

5. Conclusion

The complicated flow structure of a marine propeller wake was investigated using a SPIV technique. The tip vortices formed from the propeller tip go downstream periodically as the propeller rotates. The merging of two boundary layers developed along the propeller blades produces the viscous wake near the blade tip and propeller shaft. The trace of tip vortices contracts toward the propeller shaft up to the region of X/D = 0.5, thereafter it is contracted more due to the blade-to-blade interaction up to the region of X/D = 1.0. As the wake goes downstream and the flow interaction between wake sheet and tip vortices becomes weaker, the strength and asymmetry of tip vortices are decreased.

Strong out-of-plane motion takes place within the propeller slipstream. The direct comparison of 2-D PIV and SPIV results shows that the perspective error encountered in the in-plane velocity fields measured by 2-D PIV methods was about 5% ~ 10%. Since the out-of-plane motion in the propeller wake can reduce the propulsion efficiency, it should be considered in the optimum design process of a ship propeller.

The axial turbulence intensity is concentrated in the near-wake region and the flow energy of propeller wake is decreased as the flow goes downstream. The axial turbulence intensity distribution measured by 2-D PIV method is overestimated compared with that of SPIV method due to the out-of-plane flow motion. For accurate analysis on the tip vortices having strong out-of-plane motion in the near-wake, it is recommended to investigate the three velocity components using a SPIV technique.

Acknowledgment

The present work is supported by National Research Laboratory Program of Ministry of Science and Technology (MOST) of Korea.

References

Calcagno, G., Di, Felice, F., Felli, M. and Pereira, F., Propeller Wake Analysis Behind a Ship by Stereo PIV, Proceedings of 24th Symposium on Naval Hydrodynamics, Fukuoka, 3 (2002), 112-127.

Chesnaks, C. and Jessup, S., Experimental Characterisation of Propeller Tip Flow, Proceedings of 22nd Symposium on Naval Hydrodynamics, Washington D.C. (1998), 156-169.

Cotroni, A., Di, Felice, F., Romano, G. P. and Elefante, M., Investigation of the Near Wake of a Propeller Using Particle Image Velocimetry, Experiment in Fluids, 29 (2000), S227-236.

Lee, S. J., Paik, B. G. and Lee, C. M., Phase-Averaged PTV Measurements of Propeller Wake, Proceedings of 24th Symposium on Naval Hydrodynamics, Fukuoka, 4 (2002), 18-25.

Raffel, M., Willert, C., Kompenhans, J., Particle Image Velocimetry, Springer ISBN 3-540-63683-8, (1998).

Soloff, S. M., Adrian, R. J. and Liu, Z. C., Distortion Compensation for Generalized Stereoscopic Particle Image Velocimetry, Meas. Sci. Technology, 15 (1997), 1441-1454.

Stella, A., Guj, G., Di, Felice F. and Elefante, M., Propeller Wake Evolution Analysis by LDV, Proceedings of 22nd Symposium on Naval Hydrodynamics, Washington D.C., (1998), 171-188.

Yoon, J. H. and Lee, S. J., Direct Comparison of 2-D PIV and 3-D Stereoscopic PIV Measurements, Meas. Sci. Technology, 13 (2002), 1631-1642.

Author Profile

Sang Joon Lee: He received his master and Ph.D. in Mechanical Engineering from KAIST (Korea Advanced Institute of Science and Technology) in 1982 and 1986, respectively. In 1986 he worked as a senior researcher at KIMM. He is currently a professor in the Department of Mechanical Engineering at POSTECH after joining as an assistant professor in 1987. His research interests are quantitative flow visualization (PIV, PTV, LIF, Holography), experimental fluid mechanics, bluff body aerodynamics, microfluidics and flow control.

Bu Geun Paik: He received his master degree in Physics in 1995 from POSTECH and worked as a research engineer in Samsung Shipbuilding Company. He is a Ph.D. student at POSTECH and his research interests are ship hydrodynamics and turbulence control.